REGULAR ARTICLE

Shizuko Ichinose · Motoki Tagami · Takeshi Muneta · Ichiro Sekiya

Morphological examination during in vitro cartilage formation by human mesenchymal stem cells

Abstract The formation of the skeleton through endochondral ossification is one of the most complex processes in development. One approach to resolving this complexity is to examine simplified systems. In vitro cartilage formation by mesenchymal stem cells (MSCs) is observed when the cells are cultured as a micromass. Several studies have confirmed the molecular events, showing the usefulness of these cells as a differentiation model. We have elucidated the process of cartilage formation in MSCs from the morphological point of view by light and transmission electron microscopy and immunohistochemical examination. The morphology of the MSCs changed from spherical to spindle-shaped, and the cells aggregated and formed junctional complexes during Day 1. At Day 7, three layers were observed. The superficial zone consisted of several layers of elongated cells with junctional complexes. The middle zone was composed of apoptotic bodies, and the deep zone was occupied by chondrocyte-like cells excreting extracellular matrices. At Day 14, the middle zone had disappeared, and the chondrocyte-like cells in the deep zone were detected within cartilage lacuna. They were covered by cartilage matrices containing collagen types I, II, and X and chondroitin sulfate. By Day 21, the outer layer consisting of spindle-shaped cells had disappeared in places. As the pellet grew, the outer layer seemed to be unable to stretch to maintain a constant covering around the pellet. Our findings have thus revealed that MSCs change their morphology depending upon their microenvironment during differentiation. In vitro cartilage formation by MSCs makes it possible to clarify the detailed morphological events that occur during chondrogenesis.

S. Ichinose and I. Sekiya contributed equally to this study

S. Ichinose (✉)
Instrumental Analysis Research Center,
Tokyo Medical and Dental University,
1-5-45 Yushima, Bunkyo-ku,
Tokyo, 113-8510, Japan
e-mail: ichinose.bioa@cmn.tmd.ac.jp
Tel.: +81-3-58035792
Fax: +81-3-58030232

M. Tagami
Department of Medicine,
Sanraku Hospital,
Chiyoda-ku,
Tokyo, 101-0062, Japan
Tel.: +81-3-32923981
Fax: +81-3-32925023

T. Muneta
Center of Excellence Program for Frontier Research on
Molecular Destruction and Reconstruction of Tooth and Bone,
Tokyo Medical and Dental University,
Tokyo, Japan
Tel.: +81-3-58034586
Fax: +81-3-58030266

T. Muneta · I. Sekiya
Section of Orthopedic Surgery, Division of Bio-Matrix,
Graduate School, Tokyo Medical and Dental University,
1-5-45 Yushima, Bunkyo-ku,
Tokyo, 113-8519, Japan
Tel.: +81-3-58034586
Fax: +81-3-58030266

Introduction

The formation of the vertebrate skeleton through endochondral bone formation is one of the most complex processes in biology (DeLise et al. 2000). It begins with the migration of undifferentiated mesenchymal cells from the lateral plate mesoderm to the sites destined to become bone. One approach to resolving the complexities is to examine simplified systems in vitro.

Mesenchymal stem cells (MSCs) have multiple differentiation potentials (Prockop 1997; Pittenger et al. 1999), and in vitro cartilage formation is observed when the cells are cultured as a micromass in a defined medium for chondrogenesis (Johnstone et al. 1998; Sekiya et al. 2001). Several studies have clarified the molecular events during

the chondrocyte differentiation of MSCs and have shown the usefulness of these cells as a differentiation model (Sekiya et al. 2002; Imabayashi et al. 2003).

In this study, we have studied cartilage formation in a simplified model by morphological methods, including immunohistochemistry, transmission electron microscopy, and immunoelectron microscopy. These techniques have clarified the detailed morphological events occurring during chondrogenesis.

Materials and methods

Isolation and culture of human MSCs

This study was approved by an institutional review board of Tokyo Medical and Dental University (no. 210) and informed consent was obtained from the study subject. Humanbone marrow was aspirated from the tibial tunnel through an 18-gauge needle under spinal anesthesia during anterior cruciate ligament reconstruction surgery. To isolate nucleated cells, Ficoll (Ficoll-Paque; Pharmacia, Piscataway, N.J.) was layered beneath the bone marrow diluted with Hanks' balanced salt solution (HBSS; Invitrogen), and the layered preparation was then centrifuged at 450g for 10 min at room temperature. The mononuclear cell layer was transferred from the interface and incubated in a culture dish (Nalge Nunc International, Rochester, N.Y.) in complete culture medium: αMEM containing 20% fetal bovine serum (FBS; Invitrogen; lot selected for rapid growth of MSCs), 100 U/ml penicillin (Invitrogen), 100 μg/ml streptomycin (Invitrogen), and 250 ng/ml amphotericin B (Invitrogen). After 14 days, the cells were replated for expansion and used for experiments (Sakaguchi et al. 2004).

In vitro chondrogenesis

MSCs (200,000) were placed in a 15-ml polypropylene tube (Becton Dickinson) and centrifuged at 450g for 10 min. The pellet was cultured at 37°C with 5% CO_2 in 400 μl chondrogenic medium: high-glucose Dulbecco's modified Eagle medium (Invitrogen) supplemented with 500 ng/ml bone morphogenetic protein-2 (BMP-2; R&D Systems, Minneapolis, Minn.), 10 ng/ml transforming growth factor-β3 (TGF-β3), 100 nM dexamethasone (Sigma-Aldrich, St Louis, Mo.), 50 μg/ml ascorbate-2-phosphate, 40 μg/ml proline, 100 μg/ml pyruvate, and 50 mg/ml ITS+Premix (Becton Dickinson; 6.25 μg/ml insulin, 6.25 μg/ml transferrin, 6.25 ng/ml selenious acid, 1.25 mg/ml bovine serum albumin [BSA], and 5.35 mg/ml linoleic acid). The medium was replaced every 3–4 days for 21 days (Sekiya et al. 2005).

Transmission electron microscopy

The cultures were ended by fixing the pellets with 2.5% glutaraldehyde in 0.1 M phosphate-buffered saline (PBS) for 2 h. The cells were washed and fixed overnight at 4°C in the same buffer and post-fixed with 1% OsO_4 buffered with 0.1 M PBS for 2 h. The pellets were dehydrated in a graded series of ethanol and embedded in Epon 812. Semi-thin (1 μm) sections for light microscopy were collected on glass slides and stained for 30 s with toluidine blue. Ultrathin (90 nm) sections were collected on copper grids, double-stained with uranyl acetate and lead citrate, and then examined by transmission electron microscopy (H-7100, Hitachi, Hitachinaka, Japan; Ichinose et al. 2003a,b; Tagami et al. 2003).

Immunohistochemistry

Immediately after fixation with 4% paraformaldehyde in 0.1 M PBS for 1 h, pellets were immersed in 25% sucrose in 0.1 M PBS for 24 h at 4°C, mounted in orthochlorotoluene (OCT) embedding medium and quickly frozen in liquid nitrogen. Frozen sections thickness of 6 μm were cut on a CM1900 cryostat (Reichert, Vienna, Austria) at a knife and specimen temperature of −15°C. The frozen sections were placed on silane-coated glass slides and washed in 0.1 M PBS. For immunohistochemical staining, the sections were blocked with 0.1 M PBS containing 1% normal goat serum for 1 h at 25°C. Mouse antibody against collagen type I and type II (Fuji Yakuhin, Japan) and rabbit antibody against collagen type X (Cosmo Bio., Japan) containing 1% BSA were placed on the sections for 24 h at 4°C. These three antibodies were diluted 1:500 in 0.1 M PBS. After extensive washes with 0.1 M PBS, the sections were incubated for 30 min with biotinylated secondary antibodies. Immunostaining was detected by the Vector ABC kit with a horse antimouse antibody for collagen type I and type II and antirabbit antibody for collagen type X (Vector Laboratories, Burlingame, Calif.). Normal mouse and rabbit sera were used as negative controls. Counterstaining was performed with Mayer's hematoxylin.

Immunocryo-ultramicrotomy and evaluation

Immediately after fixation in 4% paraformaldehyde, 0.1% glutaraldehyde in 0.1 M PBS for 1 h, pellets were immersedin 2.3 M sucrose in 0.1 M PBS for 24 h at 4°C, mounted on a holder, and quickly frozen in liquid nitrogen. Frozen sections with a thickness of under 0.5 μm were cut on an ultracut S microtome (Reichert) equipped with an FCS low-temperature sectioning system (Reichert) and a knife and specimen temperature maintained at −80°C. The frozen sections were picked up from the knife on a mixture of 2.0 M sucrose in 0.1 M PBS pH 7.4 (Tokuyasu 1986), mounted on silane-coated glass, and then placed on droplets of 1% BSA in 0.1 M PBS on a Parafilm sheet for 1 h at 4°C to eliminate nonspecific binding of the antibodies. The mounted sections were subsequently transferred to droplets of mouse antibody against collagen type I or type II (Fuji Yakuhin, Japan) or chondroitin

Table 1 Quantitation of immunogold particles/μm^2 in the deep zone of micromass pellets (−; none, +; 20 particles, ++; 20–100 particles, +++; 100–200 particles, ++++; over 200 particles)

Antibody	Time in culture (days)			
	1	7	14	21
Collagen type I	+	++	+	+
Collagen type II	−	+	++	+++
Collagen type X	+	+	++	+++
Chondroitin sulfate	++	+++	+++	++++

sulfate-proteoglycans (Seikagaku Kogyo, Japan), or a rabbit antibody against collagen type X (Cosmo Bio.) for 48 h at 4°C. The dilution of antibody against collagen type I, collagen type II, collagen type X, and chondroitin sulfate-proteoglycans was 1:20, 1:20, 1:50, and 1:50 with 1% BSA in 0.1 M PBS, respectively. Each mounted section was then washed with 0.1 M PBS and incubated with goat anti-rabbit IgG or goat anti-mouse IgG+IgM conjugated with 10–15 nmΦ gold colloidal particles (diluted 1:20 or 1:50 with 1% BSA in 0.1 M PBS, respectively; British Bio Cell International, UK) for 24 h at 4°C. After incubation, the mounted sections were washed with 0.1 M PBS for 2 h. The sections were subsequently fixed in 2.5% glutaraldehyde, post-fixed in a 1% OsO$_4$ solution in 0.1 M PBS, dehydrated in a graded series of ethanol, embedded in Epon 812, stained with uranyl acetate, and examined by transmission electron microscopy (H-7100, Hitachi).

For evaluation, gold particles in 1 $\mu m \times 1$ μm of at least 20 different fields of extracellular matrix adjacent to cells were systematically counted (Bendayan et al.1980; Yokota et al. 1984; Eskelinen et al.2002). The presence of collagen type I, II, and X and chondroitin sulfate-proteoglycan was evaluated as given in Table 1.

Results

Light microscopy

Human MSCs were cultured as micromass pellets to induce chondrogenesis. At Day 0, most of the cells were round, with or without short processes. At this stage, the cells remained separated (Fig. 1a).

Fig. 1 Optical micrograph of human MSCs in micromass pellets for chondrogenesis. (**a**) Day 0. (**b**) Day 1. (**c**) Day 7. (**d**) Day 14. (**e**) Day 21 (high-power magnification). (**f**) Day 21 (low-power magnification). Toluidine blue staining
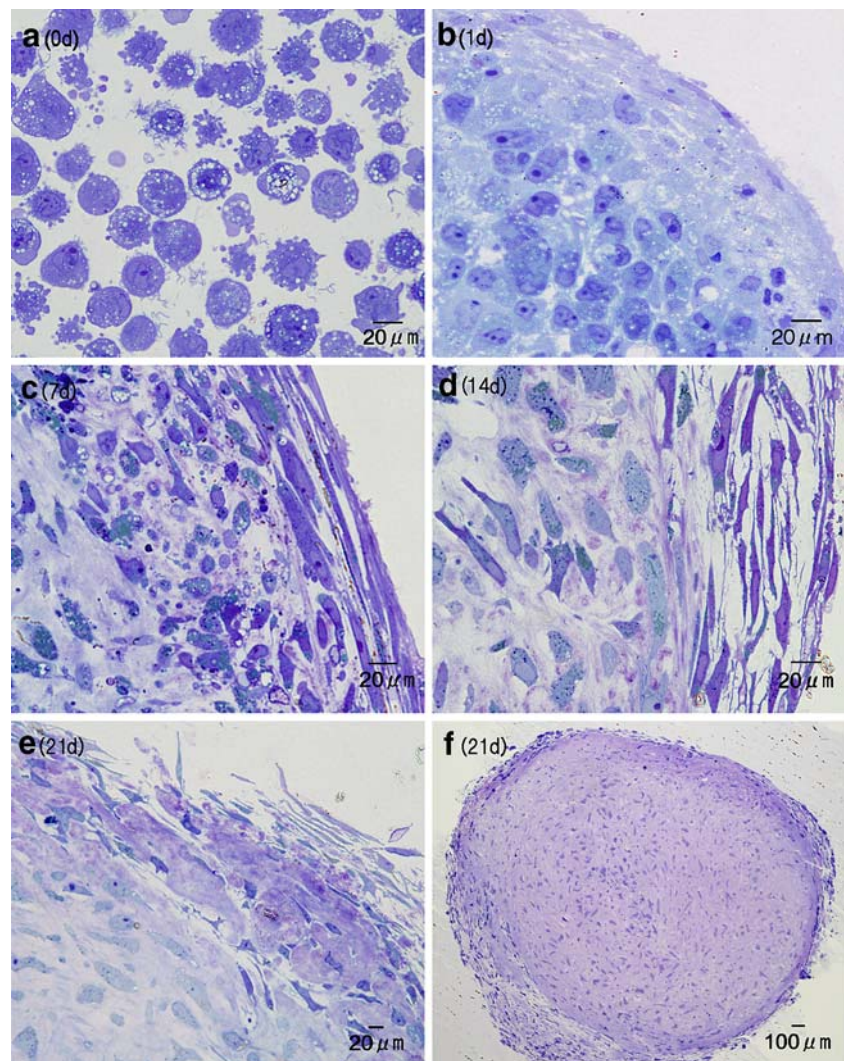
At Day 1, the cells aggregated into a micromass. The cells in the superficial zone now had a spindle morphology. Round and polygonal cells were observed in the deep zone (Fig. 1b).

At Day 7, three layers were seen in a micromass: the superficial zone, the middle zone, and the deep zone (Fig. 1c). The superficial zone consisted of four or five layers of elongated cells with a poor matrix. The cells were organized along the surface of the micromass. Smaller round and polygonal cells existed in the middle zone. Additionally, a number of small fragments, later confirmed as being apoptotic changes by electron microscopy, were observed. The deep zone contained larger polygonal cells with rich extracellular matrix.

By Day 14, the middle zone had disappeared (Fig. 1d), and the pellet had two distinctive zones: the outer and center zones. Spindle-shaped cells were present in the outer zone, and the polygonal cells lay in the center zone.

At Day 21, the outer layer consisting of spindle-shaped cells had disappeared in places. As the pellet grew, the outer layer seemd unable to stretch to maintain a constant covering around the pellet (Fig. 1e, f).

Ultrastructural examination

We examined ultrastructural changes by transmission electron microscopy on Days 0, 1, 7, 14 and 21 of culture.

On Day 0, MSCs showed a round morphology with a euchromatic and notched nucleus and a prominent nucleolus. A large number of cell processes were present at the cell surface. The cells contained well-developed organelles, including mitochondria, endoplasmic reticulum, Golgi apparatus, and large quantities of free ribosomes.
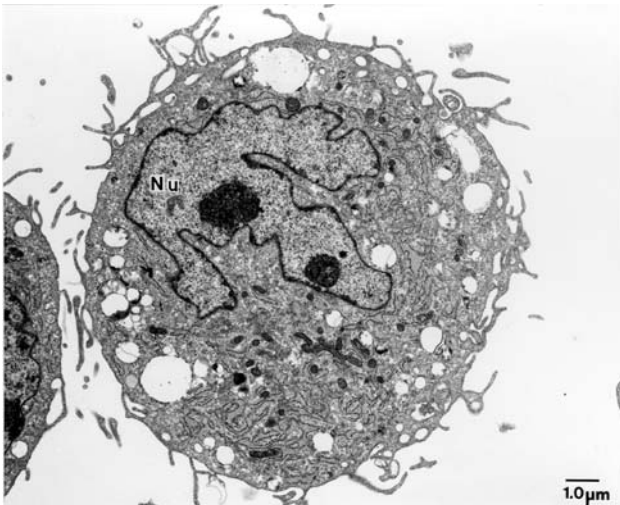

Fig. 2 Transmission electron-microscopic (TEM) image of MSC at Day 0. A round cell containing well-developed organelles, including large quantities of mitochondria, endoplasmic reticulum, Golgi apparatus, lipid droplets, and free ribosomes. Its nucleus (*Nu*) was euchromatic, notched, and filled with prominent nucleoli. A large number of cell processes were present at the cell surface

Fig. 3 TEM image of MSCs in micromass pellets at Day 1. The MSCs had lost the cell processes at the surface and produced cell–cell adherent junctions (*arrows* junctional complex at the luminal surface of MSCs); the complex shown consists of maculae adherentes (desmosomes)

Lipid droplets were also observed throughout the cytoplasm (Fig. 2).

At Day 1, the MSCs had lost the cell processes at the surface and produced cell–cell adherent junctions (Fig. 3). Junctional complexes were observed at the luminal surface of the MSCs and consisted of maculae adherentes (desmosomes).

By Day 7, the spindle-shaped cells were located at the surface. They each possessed a large euchromatic ovoid nucleus and formed junctional complexes (Fig. 4a). Many apoptotic bodies were observed in the area just beneath the surface layer; they had characteristic condensations of the chromatin (Fig. 4b). In the deep layer, the polygonal cells, each of which had an ovoid nucleus and well-developed endoplasmic reticulum, produced large 45quantities of extracellular fibers. The polygonal cells had several morphological characteristics of chondrocytes (Fig. 4c).

At Day 14, the chondrocyte-like cells lay in the deep layer and were detected within cartilage lacuna surrounded by cartilage matrices (Fig. 5a). The cells produced large amounts of extracellular matrix (Fig. 5b).

By Day 21, the chondrocyte-like cells had produced large quantities of matrix vesicles that lay around the cells (Fig. 6).

Immunohistochemistry

The expression of collagen type I was diffuse at Day 1 but was present in the three layers by Day 7, being especially strong in the superficial layer. At Days 14 and 21, the strong expression remained in the superficial layer but gradually decreased in the deep zone.

Expression of collagen type II was not observed at Day 1. At Day 7, weak expression was visible only around the middle zone. At Days 14 and 21, the expression of

Fig. 4 TEM images of MSCs in micromass pellets at Day 7. (**a**) Superficial zone. Spindle-shaped cells each with a large ovoid nucleus (*Nu*) and junctional complexes (*arrows*). (**b**) Middle zone. A number of characteristic apoptotic bodies and condensations of the chromatin were observed (*arrow* typical inclusion). (**c**) Deep zone. A polygonal cell with rough endoplasmic reticulum (*rER*), a round nucleus (*Nu*), and large quantities of extracellular fibers
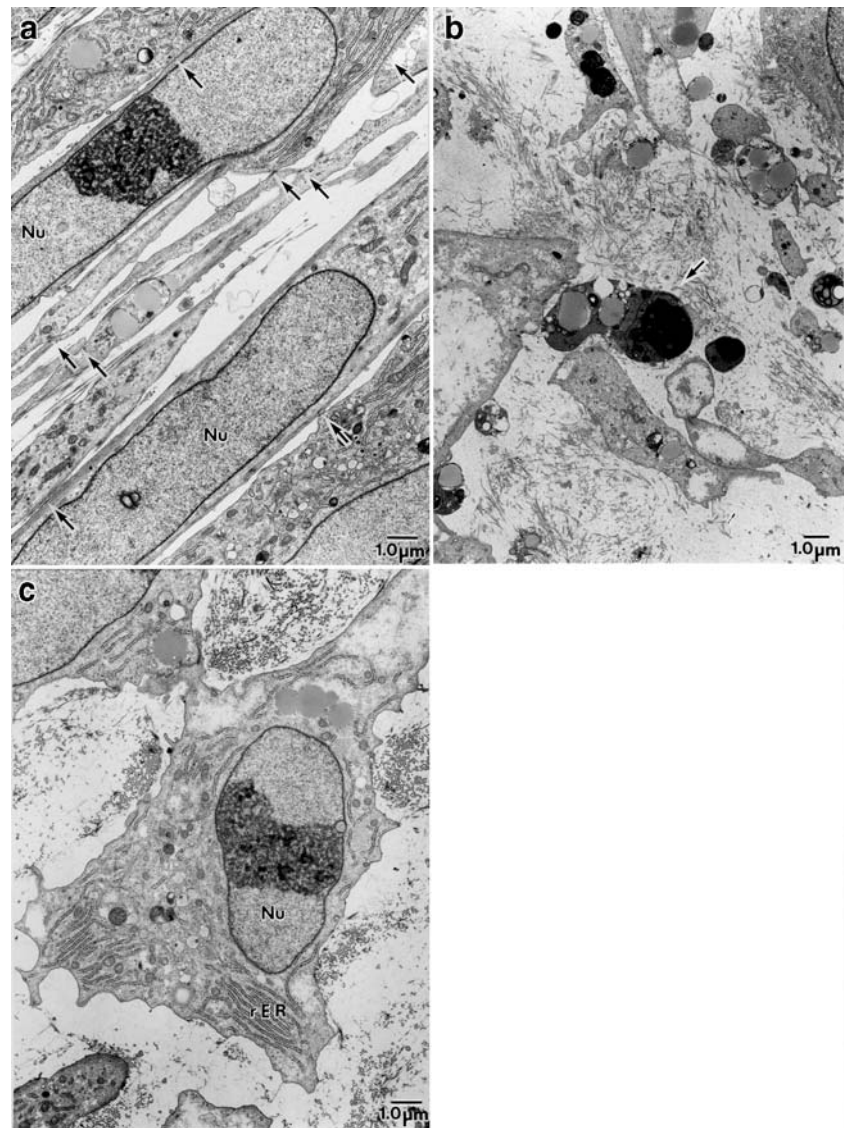
collagen type II dramatically increased in the deep zone. In contrast with collagen type I, expression of collagen type II was not detectable in the superficial zone at any time point.

Expression of collagen type X was diffuse at Day 1 and was observable in all three layers by Day 7. At Days 14 and 21, the expression of collagen type X gradually increased. No discernible difference was seen in the expression of collagen type X between the layers throughout differentiation (Fig. 7).

Immunoelectron microscopy

The localization of collagen types I, II, and X and chondroitin sulfate was indicated by gold particles with the immunoelectron-microscopy technique. We examined the extracellular matrix adjacent to the chondrocyte-like cells in micromass pellets at Days 1, 7, 14 and 21 of culture.

Expression of collagen type I (Fig. 8a), type II (Fig. 8b), and type X (Fig. 8c) and chondroitin sulfate (Fig. 8d) was visible by Day 14. The expression of collagen types I, II, and X and chondroitin sulfate during Day 1–21 was evaluated by the extent of gold particle deposition (Table 1).

Discussion

Chondrogenesis of MSCs was first observed by (Ashton et al. 1980). A defined medium for in vitro chondrogenesis by MSCs was first described by Johnstone et al. (1998) who developed micromass cultures of rabbit MSCs and supplemented the medium with both TGF-β and dexamethasone to produce cartilage. Subsequently induction of chondrogenesis in human MSCs was reported under similar conditions (Mackay et al. 1998; Yoo et al. 1998). Previously, we demonstrated that the addition of BMP-6,
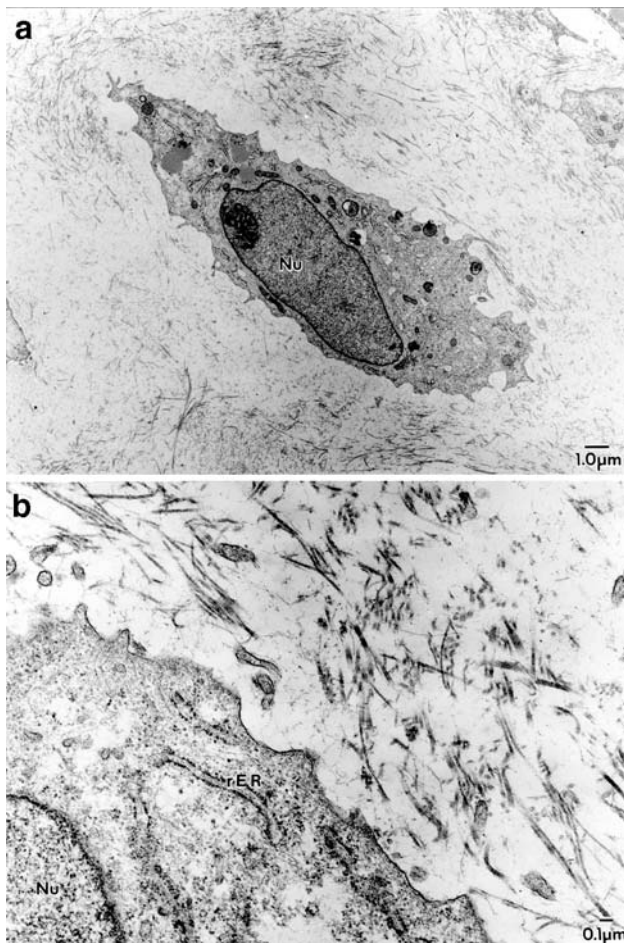
Fig. 5 TEM images of MSC in micromass pellets at Day 14. (**a**) A cell in the deep zone showing chondrocyte-like features and an irregular outline and lying within a cartilage lacuna surrounded by cartilage matrices. (**b**) A cell producing large quantities of extracellular matrix

a cytokine known to promote chondrogenesis, enhanced chondrogenesis by human MSCs (Sekiya et al. 2001) under the conditions employed by Johnstone et al. (1998). Furthermore, we defined the time sequence in gene expression during in vitro chondrogenesis in our model and demonstrated the usefulness of the model (Sekiya et al. 2002). Recently, we compared the ability of recombinant human BMP2, BMP4, and BMP6 to enhance in vitro cartilage formation of MSCs and demonstrated that BMP-2 was the most effective (Sekiya et al. 2005).

We have determined, by means of light- and electron microscopy, the morphological changes occurring during in vitro chondrogenesis by MSCs. This can be summarized as follows. At Day 1, the cells alter their morphology from spherical to spindle-shaped and aggregate with each other via junctional complexes. At Day 7, fibroblast-like cells appear in the superficial zone, apoptotic cells in the middle zone, and chondrocyte-like cells in the deep zone. At Day 14, the middle zone disappears, and by Day 21, the superficial zone begins to disappear (Fig. 9).

Our previous study showed that DNA yield per a pellet decreased and radioactivity per DNA in cells prelabeled with ^{3}H-thymidine was stable during in vitro chondrogenesis by MSCs (Sekiya et al. 2002). These results indicated that a pellet increased its size by the production of extracellular matrix, and not by cell proliferation. Our present morphological study accounts for the mechanism demonstrated previously; (1) viable MSCs decrease by apoptosis in the middle zone of micromass, (2) MSCs do not seem to divide because no features of cell mitosis have been observed, and (3) the chondrocyte-like cells produce large amount of collagen fibrils (Fig. 9).

Three methods can be used for immunoelectron microscopy: pre-embedding, post-embedding, and non-embedding, depending to the step at which the antibody is applied to the biological specimens. The non-embedding method (immunocryo-ultramicrotomy) generally provides better accessibility of antigens to antibodies and also allows more sensitive examination of the specimens than the pre- and post-embedding methods with resins. Therefore, we have employed the non-embedding method to determine the expression and distribution of collagens and chondroitin sulfate during the differentiation of MSCs in culture. In addition, gold particles within squares of extracellular matrix adjacent to the cells have been counted. We have determined the time-kinetics of chondrocyte-associated or specific proteins by using quantitative analysis of specimens obtained by immunocryo-ultramicrotomy. This study is the first to examine the differentiation process of MSCs by applying the technique of immunocryo-ultramicrotomy and quantitative analysis.

Some similarities are apparent between in vivo and in vitro chondrogenesis. Limb development during skeletal formation begins with the migration of mesenchymal cells to sites destined to become bone (Fell 1925; Summerbell and Wolpert 1972). The mesenchymal cells undergo a condensation step and then form a cartilaginous scaffold. In our system, MSCs are centrifuged to form a three-dimensional structure. This step seems to mimic the condensation step observed at the initiation of skeletogenesis.
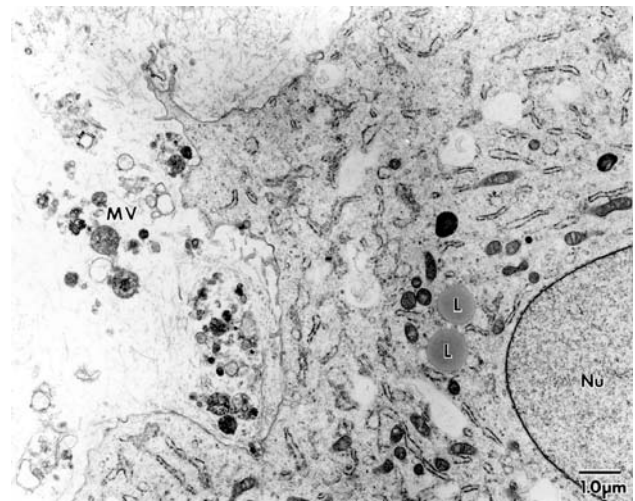

Fig. 6 TEM images of MSCs in micromass pellets at Day 21. Note the chondrocyte-like cell (*Nu* nucleus) producing large quantities of matrix vesicles (*MV*)
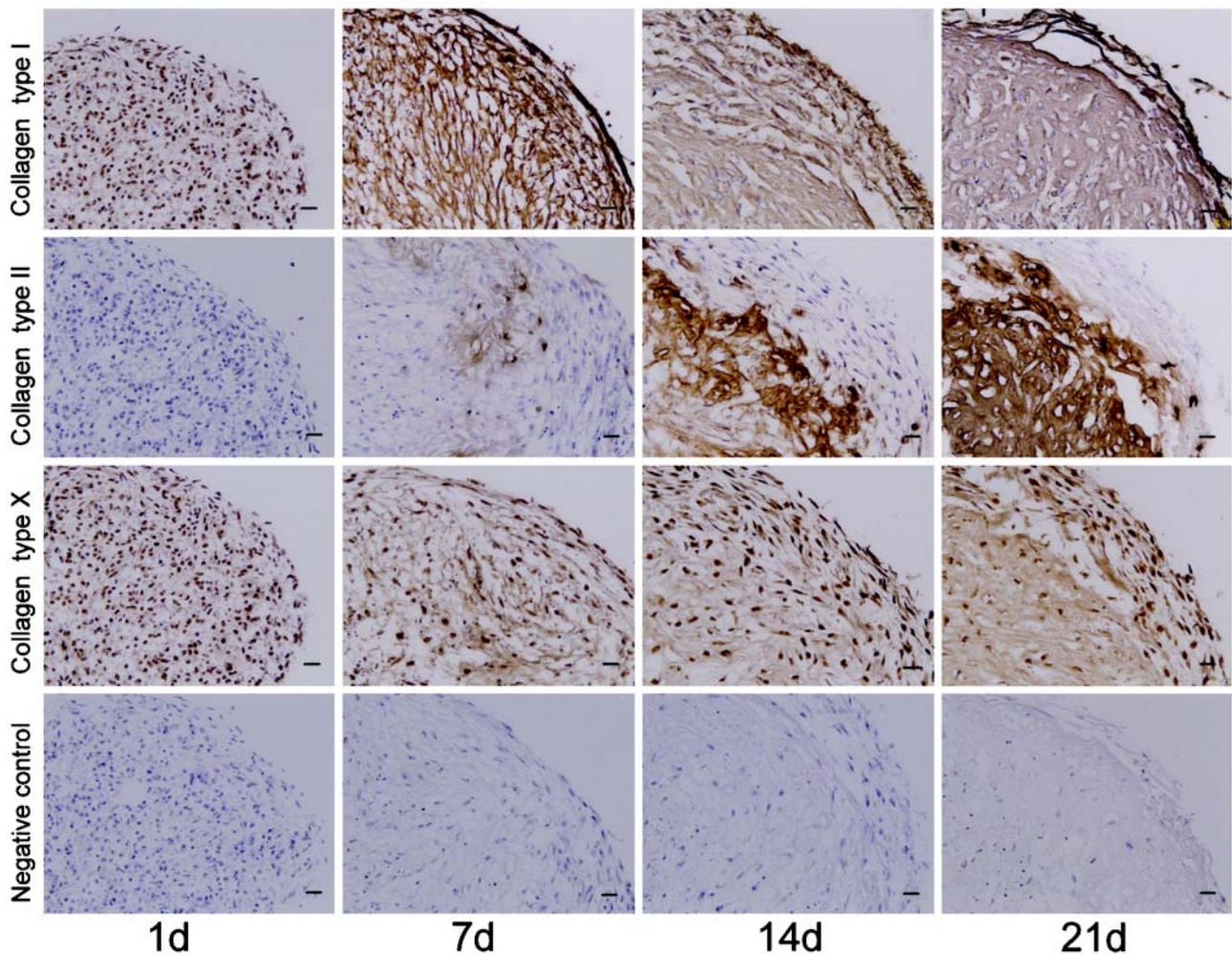
Fig. 7 Immunohistochemistry of MSCs in micromass pellets exhibitng chondrogenesis. Immunostaining for collagen types I, II, and X and the negative control without the first antibody. *Bar* 20 μm

In our experiments, when MSCs are cultured in a similar chondrogenesis medium without pellet formation, the cells do not fully differentiate into cartilage. This suggests that the condensation of MSCs plays an important role for chondrogenesis in vitro.

The condensation of mesenchymal cells observed in vivo is apparently triggered by BMP2, which induces the production of cell adhesion proteins N-cadherin and N-CAM (Edelman 1986; Oberlender and Tuan 1994). Our previous study has demonstrated that BMPs dramatically enhance the chondrogenesis of MSCs in vitro, and the effect of BMP2 is stronger than that of BMP4 or BMP6 (Sekiya et al. 2005). Interestingly, MSCs in vitro condense after centrifugation in the absence of BMP2. This indicates that exogenous BMP2 is a crucial factor for chondrogenesis after cell condensation in vitro.

During limb development, mesenchymal cells at the center synthesize an extracellular matrix that is rich in type II collagen, as has also been observed in our in vitro model (Fell 1925; Summerbell and Wolpert 1972; DeLise et al. 2000). The synthesis of the cartilaginous matrix,

which begins shortly after condensation, appears to have several molecular triggers. One key pathway/trigger is the binding of TGF-βs to their receptors, which in turn transmit signals either through a SMAD pathway or a MAP kinase pathway to activate genes for the synthesis of cartilage matrix (Shibuya et al. 1996; Ishitani et al. 1999; Meneghini et al. 1999). Our in vitro study has shown that MSCs produce cartilage without TGF-β; however, much less cartilage matrix is synthesized than in cultures with TGF-β (data not shown). The binding of TGF-βs to their receptors is one of the key triggers to activate genes for the synthesis of cartilage matrix, such as the gene for type II collagen, during in vivo cartilage formation.

One of the early nuclear events in the synthesis of the cartilaginous matrix in vivo is the expression of the *Sox 9* gene (Wagner et al. 1994; Wright et al. 1995; Lefebvre and de Crombrugghe 1998; Sekiya et al. 2000), a member of the family of Sry-type high mobility group genes (Pevny and Lovell-Badge 1997; Werner and Burley 1997). *Sox 9*, in a complex with *Sox 5* and *Sox 6*, cooperatively binds to a specific sequence in an enhancer of the *Col2a1* gene that

Fig. 8 MSCs in micromass pellets at Day 14 after immunocryo-ultramicrotomy and immunoelectron microscopy. (**a**) Collagen Type I. (**b**) Collagen type II. (**c**) Collagen type X. (**d**) Chondroitin sulfate. *Bar* 100 nm
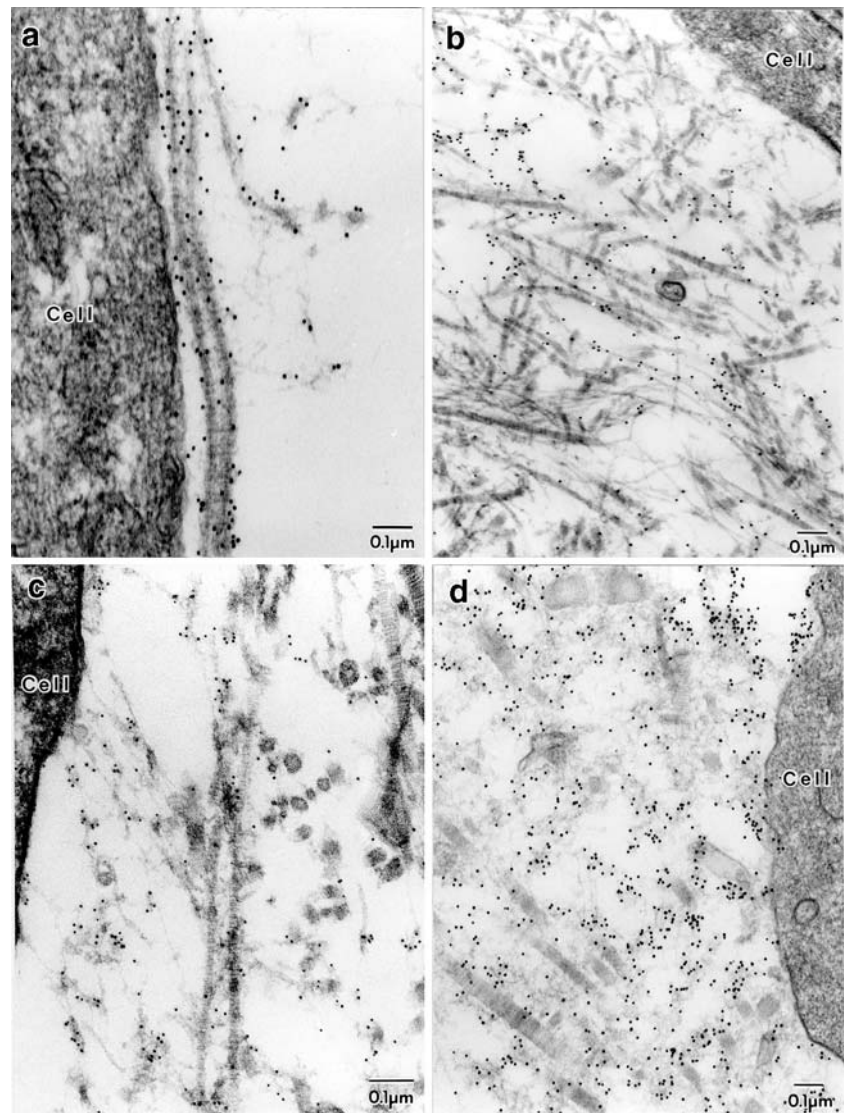
codes for type II collagen (Lefebvre and de Crombrugghe 1998). In our in vitro model of chondrogenesis, mRNA expression of SOX5, SOX6, and SOX9 increase continuously (Sekiya et al. 2005). These SOX genes are probably important transcriptional factors for both in vivo and in vitro cartilage formation.
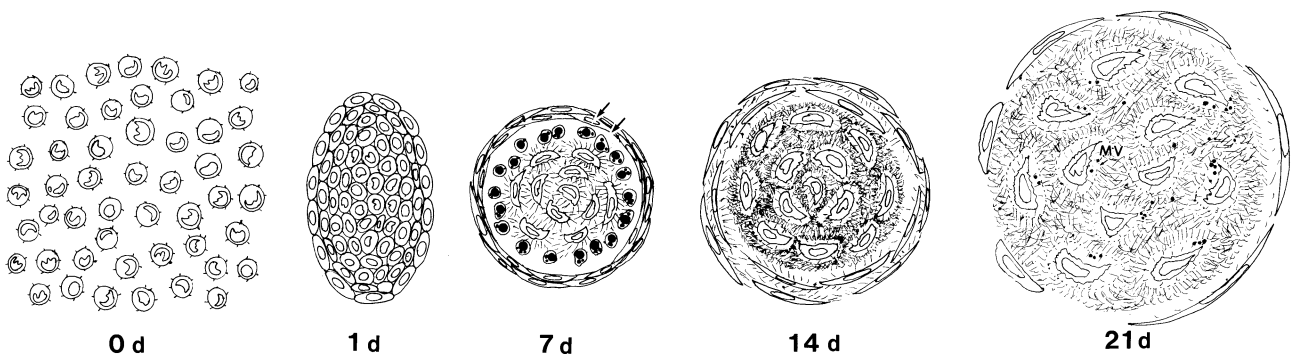

Fig. 9 Scheme for morphological events in micromass pellets during in vitro cartilage formation by MSCs. At Day 0, most of the cells are round. A large number of cell processes are present at the cell surface. At Day 1, the MSCs have lost their cell processes at the surface and produce cell–cell adherent junctions. At Day 7, fibroblasts appear in the superficial zone, apoptotic cells (*arrows*) in the middle zone, and chondrocyte-like cells in the deep zone. The chondrocyte-like cells produce large quantities of extracellular fibers. At Day 14, the middle zone disappears, and the chondrocyte-like cells in the deep zone lie within cartilage lacuna surrounded by cartilage matrices. At Day 21, the superficial zone begins to disappear. Matrix vesicles (*MV*) are present in the cartilage matrices

Little is known about the ultrastructural changes occurring during skeletogenesis in vivo. Ito and Kida (2000) have investigated the development of the rat knee joint by light and electron microscopy and have demonstrated that mesenchymal cells elongate in the presumptive tangential zone, which appears to become the surface of the joint. Round or polygonal cells remain in the presumptive transitional zone, which seems to be part of the cartilage (Ito and Kida 2000). Matsuda et al. (1997) have examined the relationship between the development of the temporomandibular joint and apoptosis. They have demonstrated apoptotic cells at the subsurface of the condyle and suggest that apoptosis plays an important role during development (Matsuda et al. 1997). Our study has shown that cartilage can be distinguished in three layers within the cultured MSC pellet and that the middle zone disappears by apoptosis. We have observed morphological similarities to in vivo chondrogenesis in that the cartilage forms distinguishable layers and apoptotic cells appear at the subsurface of the cartilage.

During limb development in vivo, chondrocytes in the cartilaginous scaffold differentiate into hypertrophic chondrocytes at the growth plate. Eventually, most of the cartilaginous scaffold is replaced by marrow and bone matrix so that the only remaining cartilage is on the articular surface and the growth plate (DeLise et al. 2000). One of the dissimilarities between the in vivo and our in vitro cartilage formation is that expression of type X collagen, a marker of the hypertrophic chondrocyte, has been observed in MSCs during the early phase and increases diffusely together with cartilage formation. This may be explained by the simplicity of our system in which the growth factors in the differentiation medium are kept at constant levels during cartilage formation.

In our system, MSCs change their morphology depending on their microenvironment throughout differentiation. After centrifugation of the MSCs, the cells form pellets and become connected with junctional complexes at Day 1. The gradient of oxygen, cytokines, or other nutrients presumably affect the fate of the cells. In vitro cartilage formation by MSCs has made it possible to clarify the detailed morphological events during chondrogenesis.

References

Ashton BA, Allen TD, Howlett CR, Eaglesom CC, Hattori A, Owen M (1980) Formation of bone and cartilage by marrow stromal cells in diffusion chambers in vivo. Clin Orthop 313:294–307

Bendayan M, Roth J, Perrelet A, Orci L (1980) Quantitative immunocytochemical localization of pancreatic secretory proteins in subcellular compartments of the rat acinar cell. J Histochem Cytochem 28:149–160

DeLise AM, Fischer L, Tuan RS (2000) Cellular interactions and signaling in cartilage development. Osteoarthr Cartil 8:309–334

Edelman GM (1986) Cell adhesion molecules in the regulation of animal form and tissue pattern. Annu Rev Cell Biol 2:81–116

Eskelinen E-L, Illert AL, Tanaka Y, Schwarzmann G, Blanz J, Figura K, Saftig P (2002) Role of LAMP-2 in lysosome biogenesis and autophagy. Mol Biol Cell 13:3355–3368

Fell HB (1925) The histogenesis of cartilage and bone in the long bones of the embryonic fowl. J Morphol 40:417–451

Ichinose S, Muneta T, Aoki H, Tagami M (2003a) TEM observation of seven retrieved total knee joints made of Co-Cr-Mo and Ti-Al-V alloys. Biomed Mater Eng 13:125–134

Ichinose S, Muneta T, Sekiya I, Itoh S, Aoki H, Tagami M (2003b) The study of metal ion release and cytotoxicity in Co-Cr-Mo and Ti-Al-V alloy in total knee prosthesis—scanning electron microscopic observation. J Mater Sci Mater Med 14:79–86

Imabayashi H, Mori T, Gojo S, Kiyono T, Sugiyama T, Irie R, Isogai T, Hata J, Toyama Y, Umezawa A (2003) Redifferentiation of dedifferentiated chondrocytes and chondrogenesis of human bone marrow stromal cells via chondrosphere formation with expression profiling by large-scale cDNA analysis. Exp Cell Res 288:35–50

Ishitani T, Ninomiya-Tsuji J, Nagai S, Nishita M, Meneghini M, Barker N, Waterman M, Bowerman B, Clevers H, Shibuya H, and Matsumoto K (1999) The TAK1-NLK-MAPK-related pathway antagonizes signalling between beta-catenin and transcription factor TCF. Nature 399:798–802

Ito MM, Kida MY (2000) Morphological and biochemical re-evaluation of the process of cavitation in the rat knee joint: cellular and cell strata alterations in the interzone. J Anat 197:659–679

Johnstone B, Hering TM, Caplan AI, Goldberg VM, Yoo JU (1998) In vitro chondrogenesis of bone marrow-derived mesenchymal progenitor cells. Exp Cell Res 238:265–272

Lefebvre V, de Crombrugghe B (1998) Toward understanding SOX9 function in chondrocyte differentiation. Matrix Biol 16:529–540

Mackay AM, Beck SC, Murphy JM, Barry FP, Chichester CO, Pittenger MF (1998) Chondrogenic differentiation of cultured human mesenchymal stem cells from marrow. Tissue Eng 4:415–428

Matsuda S, Mishima K, Yoshimura Y, Hatta T, Otani H (1997) Apoptosis in the development of the temporomandibular joint. Anat Embryol 196:383–391

Meneghini MD, Ishitani T, Carter JC, Hisamoto N, Ninomiya-Tsuji J, Thorpe CJ, Hamill DR, Matsumoto K, Bowerman B (1999) MAP kinase and Wnt pathways converge to downregulate an HMG-domain repressor in *Caenorhabditis elegans*. Nature 399:793–797

Oberlender SA, Tuan RS (1994) Expression and functional involvement of N-cadherin in embryonic limb chondrogenesis. Development 120:177–187

Pevny LH, Lovell-Badge R (1997) Sox genes find their feet. Curr Opin Genet Dev 7:338–344

Pittenger MF, Mackay AM, Beck SC, Jaiswal RK, Douglas R, Mosca JD, Moorman MA, Simonetti DW, Craig S, Marshak DR (1999) Multilineage potential of adult human mesenchymal stem cells. Science 284:143–147

Prockop DJ (1997) Marrow stromal cells as stem cells for non-hematopoietic tissues. Science 276:71–74

Sakaguchi Y, Sekiya I, Yagishita K, Ichinose S, Shinomiya K, Muneta T (2004) Suspended cells from trabecular bone by collagenase digestion become virtually identical to mesenchymal stem cells obtained from marrow aspirates. Blood 104:2728–2735

Sekiya I, Tsuji K, Koopman P, Watanabe H, Yamada Y, Shinomiya K, Nifuji A, Noda M (2000) SOX9 enhances aggrecan gene promoter/enhancer activity and is up-regulated by retinoic acid in a cartilage-derived cell line, TC6. J Biol Chem 275:10738–10744

Sekiya I, Colter DC, Prockop DJ (2001) BMP-6 enhances chondrogenesis in a subpopulation of human marrow stromal cells. Biochem Biophys Res Commun 284:411–418

Sekiya I, Vuoristo JT, Larson BL, Prockop DJ (2002) In vitro cartilage formation by human adult stem cells from bone marrow stroma defines the sequence of cellular and molecular events during chondrogenesis. Proc Natl Acad Sci U S A 99:4397–4402

Sekiya I, Larson BL, Vuoristo JT, Reger RL, Prockop DJ (2005) Comparison of effect of BMP-2, -4, and -6 on in vitro cartilage formation of human adult stem cells from bone marrow stroma. Cell Tissue Res 320:269–276

Shibuya H, Yamaguchi K, Shirakabe K, Tonegawa A, Gotoh Y, Ueno N, Irie K, Nishida E, Matsumoto K (1996) TAB1: an activator of the TAK1 MAPKKK in TGF-beta signal transduction. Science 272:1179–1182

Summerbell D, Wolpert L (1972) Cell density and cell division in the early morphogenesis of the chick wing. Nat New Biol 239:24–26

Tagami M, Ichinose S, Yamagata K, Fujino H, Shoji S, Hiraoka M, Kawano S (2003) Genetic and ultrastructural demonstration of strong reversibility in human mesenchymal stem cell. Cell Tissue Res 312:31–40

Tokuyasu KT (1986) Application of cryoultramicrotomy to immunocytochemistry. J Microsc 143:139–149

Wagner T, Wirth J, Meyer J, Zabel B, Held M, Zimmer J, Pasantes J, Bricarelli FD, Keutel J, Hustert E, et al (1994) Autosomal sex reversal and campomelic dysplasia are caused by mutations in and around the SRY-related gene SOX9. Cell 79:1111–1120

Werner MH, Burley SK (1997) Architectural transcription factors: proteins that remodel DNA. Cell 88:733–736

Wright E, Hargrave MR, Christiansen J, Cooper L, Kun J, Evans T, Gangadharan U, Greenfield A, Koopman P (1995) The Sry-related gene Sox9 is expressed during chondrogenesis in mouse embryos. Nat Genet 9:15–20

Yokota S, Tsuji H, Kato K (1984) Localization of lysosomal and peropxisomal enzymes in the specific granules of rat intestinal eosinophil leukocytes revealed by immunoelectron microscopic techniques. J Histochem Cytochem 32:267–274

Yoo JU, Barthel TS, Nishimura K, Solchaga L, Caplan AI, Goldberg VM, Johnstone B (1998) The chondrogenic potential of human bone-marrow-derived mesenchymal progenitor cells. J Bone Joint Surg Am 80:1745–1757